Dari: "ICTAP 2019" <ictap2019@gmail.com>
Tanggal: 5 Okt 2019 20:46
Subjek: ICTAP 2019 INFO
Kepada: <bagussapto.m@gmail.com>
Cc:

Dear Dr. Bagus,

Based on the decision of the reviewers and the editors, your manuscript entitled **Determining the temperature at each well depth as a basis for estimating hydrocarbon maturation using the well logging and thermal methods:** is ACCEPTED with REVISION.

With this e-mail, we include the template and the results of the review, **please check the plagiarism of the manuscript** and then, please revised the manuscript according to the template and the comments from the reviewer.

Kindly send your revised results by October 8, 2019

Sincere Regards

Roniyus Marjunus

CERTIFICATE

The committee of

The 9th International Conference On Theoretical And Applied Physics

Certifies

Bagus Sapto Mulyanto

as

Presenter

Bandar Lampung, Indonesia
26th - 28th September 2019

Prof. Dr.-Ing Mitra Jamal
Chairman of Physical Society of Indonesia

Dr. rer. nat. Roniyus M., S. Si, M. Si
Chairman of Committee

Journal of Physics: Conference Series

Volume 1572

2020

Previous issue Next issue

The 9th International Conference on Theoretical and Applied Physics (ICTAP) 26-28 September 2019, Bandar Lampung, Indonesia

Accepted papers received: 05 June 2020
Published online: 14 July 2020

Open all abstracts

Preface

IOP Conference Series publication procedure

Overview of the publication procedure

The following notes provide a summary of the IOP Conference Series publishing process.

1. Submit a quote request online, or contact us directly with details of the conference.
2. The IOP Conference Series team will review the details of your conference and write to confirm if we can offer a proceedings publishing contract.
3. Conferences must register to use our proceedings management platform to handle the peer review process. Each conference will have its own account and dedicated area on the platform.
4. The organizers must inform authors of the IOP Proceedings Licence.
5. Authors submit their papers to the conference organizers via the proceedings management platform and conference organisers act as editors managing the peer review process. Once review of the papers is completed the conference organizers submit the final papers to IOP Conference Series with a single click. Papers submitted to IOP Publishing must be in PDF format and in their final version ready for publication. IOP Publishing does not edit or proofread papers after they are submitted. Please ensure that any changes have been approved by authors prior to the PDFs being submitted to IOP Publishing.
6. Production and publication. We will process the PDFs into a format suitable for publication and upload them to our pre-publication servers. The communicating editor will be sent a username and password to access that server to make a final check of the proceedings before final publication. Please note the following important points:
   - Once a paper has been published online, changes will only be permitted in cases of serious scientific error. In those cases, an erratum or corrigendum will be published according to the standard practices of professional scientific publishing.
   - Change requests relating to stylistic issues cannot be made to proceedings once they are published, so it is important that authors and organizers ensure papers have been adequately checked and proofread prior to submission.
7. Upon publication we will write to authors (who have supplied an e-mail address) informing them of publication and providing them with a link to their paper.
8. Printed copies (if required) are provided by Curran Associates.

Journal of Physics: Conference Series

Table of contents

Volume 1572

2020

Previous issue Next issue

The 9th International Conference on Theoretical and Applied Physics (ICTAP) 26-28 September 2019, Bandar Lampung, Indonesia

Accepted papers received: 05 June 2020
Published online: 14 July 2020

Papers

OPEN ACCESS 012070

The development of multi-representation media based on instagram on temperature and heat materials

A Jatmiko, M Mila, I Irwandani, C Anwar, A Taher and P M Sari

+ Open abstract View article PDF

OPEN ACCESS 012071

The effect of Ag on thermoelectric performance of $Cu_{1-x}Ag_xS$ tetrahedrite/Al prepared using modified polyol methods

D Aditya, A S Rizky, T Suprayogi, C I Yogihati, M Diantoro, Sunaryono and S M Said

+ Open abstract View article PDF

OPEN ACCESS 012072

The effect of annealing temperature thin films indium doped SnO_2 to optics properties and material composition

A Doyan, Susilawati, S Hakim, L Muliyadi and M Taufik

+ Open abstract View article PDF

OPEN ACCESS 012073

The effect of blended learning setting on students' critical thinking skills in physics

W Suana, W S A Ningsih, N Maharta and N M A A Putri

+ Open abstract View article PDF

OPEN ACCESS 012074

The effect of chemical commitments with exposure to gamma irradiation dosage and save time on test attraction and pullet limits of HDPE pack

I Ratna, Y Soenarto and H Seputera

+ Open abstract View article PDF

OPEN ACCESS 012075

The effect site analysis based on microtremor data using the Horizontal to Vertical Spectral Ratio (HVSR) method in the Bandar Lampung City

N Haerudin, Rustadi, F Alami and I B S Yogi

+ Open abstract View article PDF

OPEN ACCESS 012076

The enhanced of photoresponse of ZnO nanorods film-coated by Cu_2O

S Maryam, A S P Dewi, N Mufti, A F Muyasaroh, A Taufiq, A Hidayat and Sunaryono

+ Open abstract View article PDF

OPEN ACCESS 012077

The enhanced performance of piezoelectric nanogenerator by increasing zinc precursor concentration during the growth of ZnO nanorods on stainless steel foil

N Mufti, A S P Dewi, M I Sanusi, A Taufiq, A Hidayat and Sunaryono

+ Open abstract View article PDF

OPEN ACCESS 012078

The influence of students' score by compare learning model auditory intelectually repetition and visualization auditory kinestetic of wave and vibration materials in SMP Negeri 33 Bandar Lampung

S Latifah, W Anggraini and O Tamara

+ Open abstract View article PDF

OPEN ACCESS 012079

The influence of TiO_2 film thickness in Dye-Sensitized Solar Cells (DSSC) performance based on TiO_2/Ag@TiO_2-ZnO

M F Rahman, Nasikhudin, A Hidayat and M Diantoro

+ Open abstract View article PDF

OPEN ACCESS 012080

The method for quantitative magnetic resonance imaging of agar phantom with contrast agent

Y Dwihapsari, E Asdiantoro and N Maulidiyah

+ Open abstract View article PDF

OPEN ACCESS 012081

The potential of the composite membranes Ch-AgNP to recover silver from X-ray film processing wastes

N N Rupiasih, W G Suharta, M Sumadiyasa, D D Fernanda and M Y Imas

+ Open abstract View article PDF

OPEN ACCESS 012082

The prospective ethnopedagogy-integrated STEM learning approach: science teacher perceptions and experiences

Abdurrahman, F Ariyani, N Nurulsari, H Maulina and I Sukamto

+ Open abstract View article PDF

OPEN ACCESS 012083

The prospective of STEM education: students' perceptions about the role of interest growth in science literacy

N Aini, T Jalmo and Abdurrahman

+ Open abstract View article PDF

OPEN ACCESS 012084

The prospective science teaching material based on Integrated-STEM approach: Analysis of teachers and students expectations

M I Sari, Abdurrahman and T Jalmo

+ Open abstract View article PDF

OPEN ACCESS 012085

The thickness effect to optical properties of SnO_2 thin film with doping fluorine

Susilawati, A Doyan, L Muliyadi, S Hakim and M Taufik

+ Open abstract View article PDF

OPEN ACCESS 012086

The use of teaching semiotic vectors in the introduction to physics

A H Mondolang, C Poluakan and S W Mongan

+ Open abstract View article PDF

OPEN ACCESS 012087

Time variations in Galactic cosmic rays as measured from Southeast Asia

D Ruffolo

+ Open abstract View article PDF

OPEN ACCESS 012088

Validation of audio-based solar system visual aid for special school students

F Widiyatun, R A Sumarni, I A D Astuti, Y B Bhakti, I Y Okyranida and D Dasmo

+ Open abstract View article PDF

OPEN ACCESS 012089

Vector in a graph line, is it important to teach physics?

C Poluakan, A Mondolang and S Mongan

+ Open abstract View article PDF

OPEN ACCESS 012090

Void ratio effect on dynamic shear modulus and shear wave velocity for soil stiffness in Banda Aceh and Aceh Besar

M Munirwansyah, R P Munirwan, V Listia, H Munirwan and Z Melinda

+ Open abstract View article PDF

OPEN ACCESS 012090

Void ratio effect on dynamic shear modulus and shear wave velocity for soil stiffness in Banda Aceh and Aceh Besar

M Munirwansyah, R P Munirwan, V Listia, H Munirwan and Z Melinda

+ Open abstract View article PDF

OPEN ACCESS 012091

Z-generation learner characteristic and expectation in the RI 4.0 era: a preliminary research in physics teacher college in Lampung

H Maulina, A Abdurrahman, I Sukamto, N Kartika and N Nurulsari

+ Open abstract View article PDF

Porosity and permeability prediction using pore geometry structure method on tight carbonate reservoir

Porosity and permeability prediction using pore geometry structure method on tight carbonate reservoir

B S Mulyanto[1], O Dewanto[1], A Yuliani[1], A Yogi[2] and R C Wibowo[1*]

[1] Geophysical Engineering Department, Engineering Faculty, Universitas Lampung, Prof. Soemantri Brodjonegoro Street No.1, Bandar Lampung, Indonesia 35145
[2] Geological Survey Center of the Ministry of Energy and Mineral Resources Diponegoro Street No.57, Bandung, Indonesia 40115

Corr. Author: rahmat.caturwibowo@eng.unila.ac.id

Abstract. Porosity and Permeability is an essential petrophysical parameter of hydrocarbon reservoirs for oil and gas production. It's can be immediately measured using cores taken from the reservoir in the laboratory and deal with the high cost. Many empirical, statistical, and intelligent approaches were suggested to predict permeability in un-cored wells based on wireline logs. The main objective of this study is to predict the porosity and permeability values in a tight carbonate reservoir. In this study, the calculation of permeability was done using the Schlumberger, East, Morris Biggs Oil, Morris Biggs Gas, and PGS (Pore Geometry Structure) methods based on core, logs, and CT-Scans data. The determination of porosity values from CT-Scan performed on 20 core plugs from two data cores, each core plugs was plotted as many as 15 points. The output is the CT-Porosity value that will be used for the distribution of predictions of PGS permeability. Based on the result, porosity and permeability range value from 5 – 11%; 0.015 – 24.5 mD and presents a poor to fair reservoir quality.

Keywords: porosity, permeability, CT-Scan, CT-Porosity

1. Introduction

Determination of reservoir rock properties is very important to better understand reservoirs. Some of these rock properties are porosity and permeability. Permeability plays an important role in the early life of the oil field and in carrying out reservoir characterization and description for reservoir management purposes because production is very dependent on permeability.

Permeability calculation methods can be done using the Schlumberger, East, Morris Biggs Oil, Morris Biggs Gas methods and pore geometry structure (PGS). In determining the permeability value by the log method, using some log data in the form of gamma-ray log, resistivity, and neutron porosity hydrogen index (NPHI) and density (RHOB). Based on these log data, petrophysical analysis can be done in the form of determining porosity (Ø), water saturation (Sw), permeability (k), and shale content (Vsh).

The amount of shale content in Indonesia is very large, so it is expected that in the next few years there will be many sources of oil and gas. It takes a long time to wait for the process of changing shale material into oil and gas [3].

Previous research by raising the theme of rock type determination and permeability prediction made by Permadi and Wibowo (2013), that the geological and reservoir engineering aspects were highly considered. Where it is known that the geometry and pore structure can be applied in rock typing as well as being the basis in calculating permeability predictions [10]. The results of this research show that there is a close relationship between the similarity of pore architecture with similar geology (lithofacies and diagenesis).

Yogi (2018) said, the method used in determining rock type will greatly affect the results of permeability calculations [12]. Permeability is the result of geological processes so that each type of rock in a reservoir has a unique permeability-porosity character. Therefore, determining the rock type must be done using the right method, so that the predicted value of the permeability will be close to the real permeability value. The method that can be used to predict the value of permeability is the PGS approach. The PGS method is very good for grouping rock types, because the geometry distribution and pore structure, where the geometry and pore structure (pore architecture) is very influential in porosity and will be related to the results of prediction of permeability. Besides, in this method, the equation is obtained from the correlation of porosity, permeability, and irreducible water saturation (Sw_{irr}).

The purpose of this study is to determine and analyze the value of permeability using the PGS method based on CT-Scan data and compared with other methods.

2. Geology

The North West Java Basin consists of two areas namely onshore and offshore in the north and south of the Java island. All areas are dominated by extensional faults with very little compressional structure. The basin is dominated by rift-related to faults which several depocenter structures (half-graben), the main depocenter being the Arjuna Sub-Basin and Jatibarang Sub-Basin. Other depocenter are Ciputat Sub-Basin and Pasirputih Sub-Basin. The depositors are dominated by tertiary sequences with thicknesses exceeding 5500 m. Important structures in the basin consist of various height areas associated with faulted anticline and horst block, folds on the descending part of the main fracture, keystone folding and striking at top of basement high. Compressional structures only occur at the beginning of the formation of the pre-rift in a relatively northwest-southeast direction in the Paleogene period [1]. The basement rocks in this basin are andesitic and basaltic igneous rocks which are in the Middle Cretaceous to Upper Cretaceous and Pre-Tertiary metamorphic rocks [11].

3. Pore Geometry Structure (PGS)

Well Logging is a method used to measure physical parameters in various boreholes to the depth. Petrophysical analysis can be applied to determine and evaluate the formation in the form of porosity, water saturation, and permeability that will be used to determine the next stage of exploration and production [6].

Permeability is indicated by k expressed in mD (milidarcy), which is the ability to flow from formation fluids. Permeability is very dependent on the grain size of the rock [5]. In the Log data, the permeability of a rock depends on the porosity and water saturation and can be calculated using equation 1 below:

$$k = a \frac{\emptyset_{eff}{}^{b}}{Sw^{c}} \quad (1)$$

where k (mD); $\emptyset_{eff}$ is the effective porosity (fraction); Sw (fraction); a is a constant (Schlumberger = 10000, Morris Biggs Gas = 6241, Morris Biggs Oil = 62500, East = 8581); b is a constant (Schlumberger = 4.5, Morris Biggs Gas = 6, Morris Biggs Oil = 6, East = 4.4); c is a constant (Schlumberger = 2, Morris Biggs Gas = 2, Morris Biggs Oil = 2, East = 2).

In the PGS method, there are 2 stages: identification of the flow unit and prediction of permeability. According to Yogi (2018), Integration of data from routine cores, special cores, and geological

descriptions can be used to group rock types (rock typing) [12]. Classification of rock types based on lithofacies and secondary porosity is based on the correlation between lithofacies, pore geometry and pore structures (pore architecture). Pore geometry or known as the average hydraulic radius is denoted by $\left(\frac{k}{\emptyset}\right)^{0.5}$, while the pore structure that explains all the internal structural features of the pores is denoted by $\frac{k}{\emptyset^3}$. The relationship between pore geometry and pore structure is shown in equation 2 below:

$$\left(\frac{k}{\emptyset}\right)^{0.5} = \emptyset \; x \left(\frac{k}{\emptyset^3}\right)^{0.5} \tag{2}$$

or,

$$\left(\frac{k}{\emptyset}\right)^{0.5} = \frac{V_p}{V_b} \; x \left(\frac{k}{\emptyset^3}\right)^{0.5} \tag{3}$$

Plotting data $\left(\frac{k}{\emptyset}\right)^{0.5}$ as the dependent variable to $\frac{k}{\emptyset^3}$ as an independent variable on the log-graph will produce a straight line with a positive slope of 0.5 and $v_p/v_b = 1$. By treating porous media as capillary tubes smooth winding and has a very small wall thickness, can be derived as Kozeny's equation. In addition, the term $\left(\frac{k}{\emptyset}\right)^{0.5}$ in the above equation implies that the medium is treated as a single fine capillary tube having $\emptyset = 1$. This condition will cause fluid to flow with flow efficiency 1, meaning that there is no delay in fluid flow at any point in the medium. Therefore, Equation 2 can represent an ideal model of porous media having a very simple geometry and pore structure.

When dealing with real porous rocks, the presence of micro, meso, and macropores, pore contractions, pore differences, and pore wall roughness will make fluid flow away from the ideal situation [4]. The speed of fluid flowing can vary significantly from one pore location to another flow stagnation and even occurs at the dead-end if possible, under real and complex conditions. In other words, the volume of fluid flowing per unit time from one position to another will be different. Therefore, it is expected that the flow efficiency will be smaller than 1. The following is the rock type equation for the real porous rock shown in equation 4:

$$\left(\frac{k}{\emptyset}\right)^{0.5} = a \left(\frac{k}{\emptyset^3}\right)^{b} \tag{4}$$

where constant a is flow efficiency and exponent b is able to represent pore complexity [10].

In addition to porosity, irreducible water saturation will also affect the results of the calculation of permeability. Where permeability will be inversely proportional to irreducible water saturation and directly proportional to porosity. Based on the relationship of the three parameters, permeability determination can be done by getting an equation between permeability and water saturation then substituted on each rock type equation. The following is a general form of the equation between permeability, porosity, and irreducible water saturation [12]:

$$Sw_{irr} = M \; k^{-n} \tag{5}$$

substituting equation 5 to $\sqrt{\frac{k}{\emptyset}}$ produces:

$$\sqrt{\frac{k}{\emptyset}} = \left(\frac{M}{Sw}\right)^{\frac{0.5}{n}} \tag{6}$$

substitute equation 4 to equation 6 will be:

$$\left(\frac{M}{Sw}\right)^{\frac{0.5}{n}} = a \left(\frac{k}{\emptyset^3}\right)^{b} \tag{7}$$

$$k = \left(\frac{M^{\frac{0.5}{n}}}{a}\right)^{\frac{1}{b}} x \left(\frac{\emptyset^{3-\frac{0.5}{b}}}{Sw^{\frac{0.5}{nb}}}\right) \tag{8}$$

The final equation of the relationship between porosity, permeability, and irreducible water saturation that will be used in the calculation of permeability as PGS permeability is shown in equation 9 below:

$$k = c\left(\frac{\emptyset^A}{Sw^B}\right) \quad (9)$$

with,

$$A = 3 - \frac{0.5}{b} \quad (10)$$

$$B = \frac{0.5}{nb} \quad (11)$$

$$c = \left(\frac{M^{\frac{0.5}{n}}}{a}\right)^{\frac{1}{b}} \quad (12)$$

4. Methods

The stages of data processing in this study are as follows: 1) calculation of the permeability value of the log data; 2) determination of rock type based on geological description; 3) determining the final permeability equation with the PGS approach; 4) distributing PGS from CT Porosity data; and 5) analyzing the results of the permeability calculations from the log data, cores, and PGS methods.

The data used in this study are: AY-7 well core rock samples of 2 cores have 54 total plugs. Core 1 has 25 plugs at a depth of 1776.00 m - 1785.80 m and Core 2 has 29 plugs at a depth of 1929.18 m - 1939.08 m; Routine core data used are porosity and permeability. While the SCAL (Special Core Analysis) data used are irreducible water saturation; CT Scan data obtained from the CT number plotting of 15 points, has a total plot point of 286 points; Log data consisting of gamma-ray log, caliper, spontaneous potential, resistivity (LLD, LLS and MSFL), neutron porosity hydrogen index (NPHI), and density (RHOB).

5. Porosity prediction

Interpretation of wells carried out at well AY-7 with a depth of 1776.00 - 1785.50 m has a thickness of 9.5 m (Zone 1) and 1929.18 - 1939.18 m has a thickness of 10 m (Zone 2). The shale volume parameter used for calculations on the AY-7 Well is the gamma-ray log, where the sand baseline value is located at the GRmin value and the shale baseline value is at GRmax respectively 149.94 gAPI and 11.19 gAPI. Based on the calculation of shale volume that has been done, the result of Vsh calculation in Zone 1 is 5.43 - 63.55% while in Zone 2 it is 1.60 - 14.51%.

Porosity is calculated by involving pre-calculated Vsh parameters and NPHI logs. Results Calculation of total porosity (PHIT) and effective (PHIE) in Zones 1 and 2 of AY-7 wells: for Zone 1, PHIT and PHIE are 11.32% and 4.99%, respectively. Whereas for Zone 2, PHIT and PHIE were 5.08% and 3.88%, respectively. The calculation results show that the PHIT value is greater than the PHIE value, this indicates that the porosity in the reservoir is not interconnected.

Water resistivity is a value of the type of water resistance to electric current. Determination of the value of water resistivity can use the Pickett plot method by crossing the curve between PHIE (effective porosity) and Rt (formation resistivity; reading from the LLD Log curve), then drawing a line on the collection of the most points so that the Rw value is obtained. The Rw value obtained from the LLD/PHIE cross-plot is 0.373 ohm.m, with values a, m, and n respectively 1, 1.24, and 1.9.

Based on the regional geological review of the study area, the constituent lithology in the research target formation is the intersection between limestone and shale and sandstone and shale interchange. This shows that the formation of the research target cannot be said to be a clean zone, due to shale interruption. And the results of the calculation of the volume of impurity (volume of shale) that have been done previously showed quite large results, which is 1-28%. Therefore, the calculation of water saturation is done using the Simandoux Equation. Where the parameters used are effective porosity (Ø

eff), formation water resistivity (Rw), formation resistivity (Rt) readings from the LLD log curve, shale resistivity (Rsh), and shale volume.

A large water saturation value is not good in a reservoir, because if the water saturation is large it will indicate that the zone has a lot of water content. This will affect the economics of a reservoir. In this study, obtained the saturation value of Zone 1 water is smaller than the dominant Zone 2 value of 100%.

6. Permeability prediction

Permeability is calculated not only using the PGS method, but using 4 other permeabilities (log permeability), namely Schlumberger, East, Morris Biggs Oil, and Morris Biggs Gas. Of the four permeabilities and validated with core data, accurate results for Zone 1 are Morris Biggs Gas permeability and Zone 2 is Timur permeability.

According to Koesoemadinata (1980), the quality of permeability in a reservoir is divided into 4 categories, namely: less than 5 mD is said to be tight; 5-10 mD is said to be sufficient (fair); 10-100 mD is said to be good, 100-1000 mD is said to be very good [7]. Based on these categories, the results of permeability calculations in Zones 1 and 2 of AY-7 Well can be categorized into tight permeability where the value is less than 5 mD. The final display of log permeability calculations can be seen in figures 1 and 2.

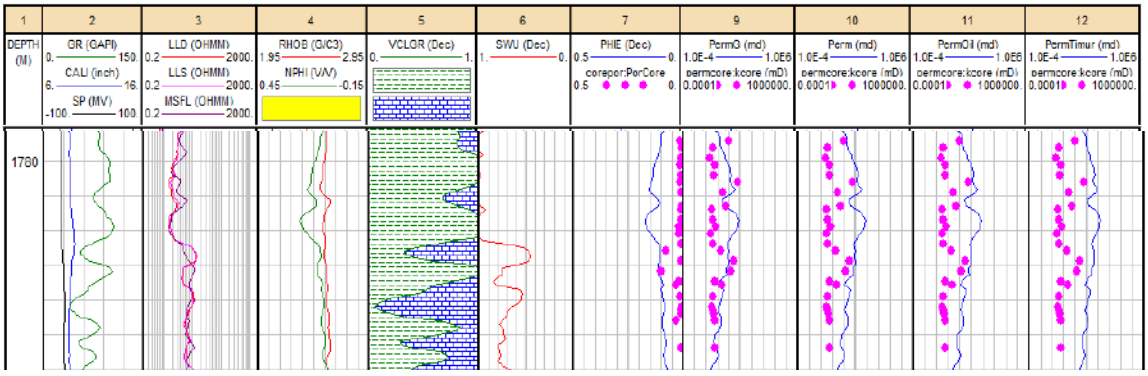

Figure 1. Quantitative Interpretation results of permeability in Zone 1

According to Listiyowati (2018), CT values represent similarities with gray levels. Color-coded reconstructions where darker colors can be indicated as areas of low density, and indicate pores filled with air [8]. Gray level can indicate CT value, for the dark gray level is identified as pore and has a low CT value. Black image shows pore (air), gray indicates low density of solid matrix, and bright white indicates higher density of solid matrix [2].

The porosity of CT is obtained from plotting CTnumber values using *VoxcelCalc Plus v8.23a* software as many as 15 points per one data scanning results (along 1 m). The purpose of this plotting is to obtain the porosity value of the results from CT, then correlate with the core porosity value and then analyze the accuracy of the values. This CT porosity data will be used to determine the distribution of PGS at each plotting point in the prediction of permeability with the PGS approach.

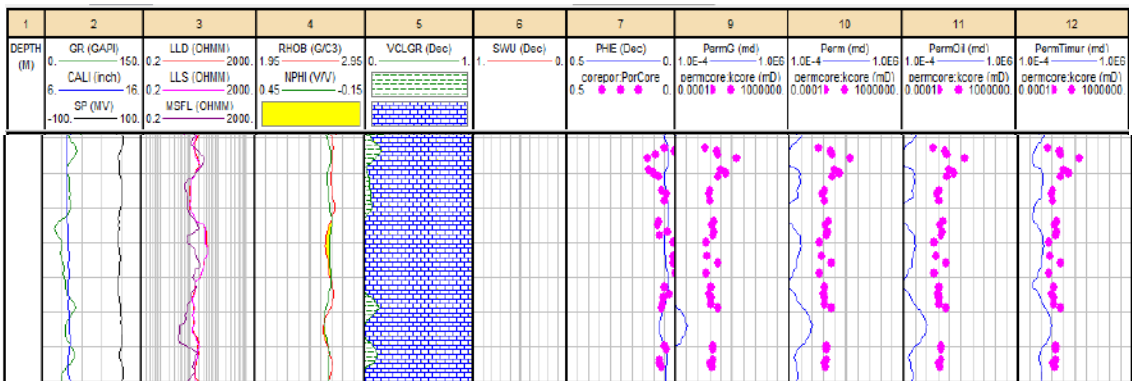

Figure 2. Quantitative Interpretation results of permeability in Zone 2

The CT porosity calculations results do not differ significantly, it can be said the difference is still within reasonable limits. However, there are still some points that are a little far from the core porosity value. This difference is due to the fact that when plotting zones each point is not the same size, so that if the zone is too large the porosity will be calculated too. In addition, when encircling the zone of the tube cover the top depth section. Close this depth is made of metal, if at the time of the zone plot of the CTnumber value is large so that the calculated porosity will also be large.

6.1. PGS approaches

In permeability prediction, the empirical correlation obtained is the same as the theoretical derived equation for capillary tube models except the strength of the pore hydraulic diameter of less than 2. Based on this, it can be seen that the capillary model can be used as an approach to characterize pore geometry and pore structure because the effective hydraulic diameter (pore geometry) derived can reflect the structure of the pore system. This model can also be used to identify rock types [9].

In this study, the grouping of rocks was carried out using the PGS method and was based on the use of the PGS rock type curve. Rock type curve is obtained from the correlation between geological description, pore geometry and pore structure in log-log charts. This will show the character of rocks in each rock type, where the greater the geometric value and pore structure, the quality of a rock will be better. figure 3 is a plot result curve between geometry and pore structure.

The figure shows the classification results based on rock texture or grain size. Can be seen in the figure, the grain size classification shows a complex distribution. There are 2 main divisions of grouping of rocks, namely: the first group that is in a green circle, shows that these rocks have the same characteristics, namely shaly limestone. Group 2, which is in a blue circle, shows similar characteristics, namely shaly limestone with stylolite. Seen in each circle there are several points that are outside the area or not the area (deviating from the group), for data that are in a green circle due to that point there is no stylolite. While the data which is in the blue circle is caused because at that point there are stylolite and fractures.

Next, determine the final rock type in the PGS curve. Of the 2 groups of rock types, they are grouped again with their geological description characteristics such as rock names, grain size, and mineral types. The results of determining the rock type on the PGS curve are shown in figure 4.

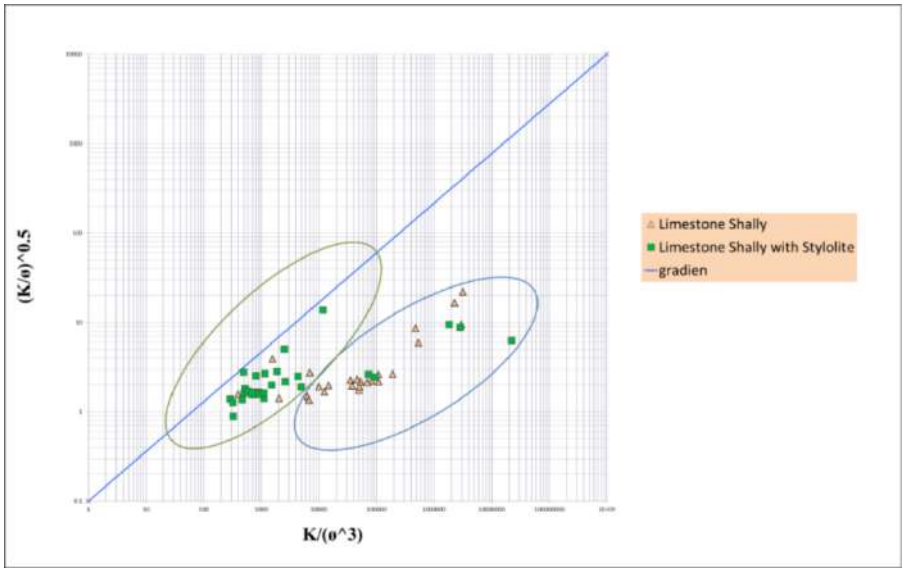

Figure 3. Item Size Plots on the PGS Curve

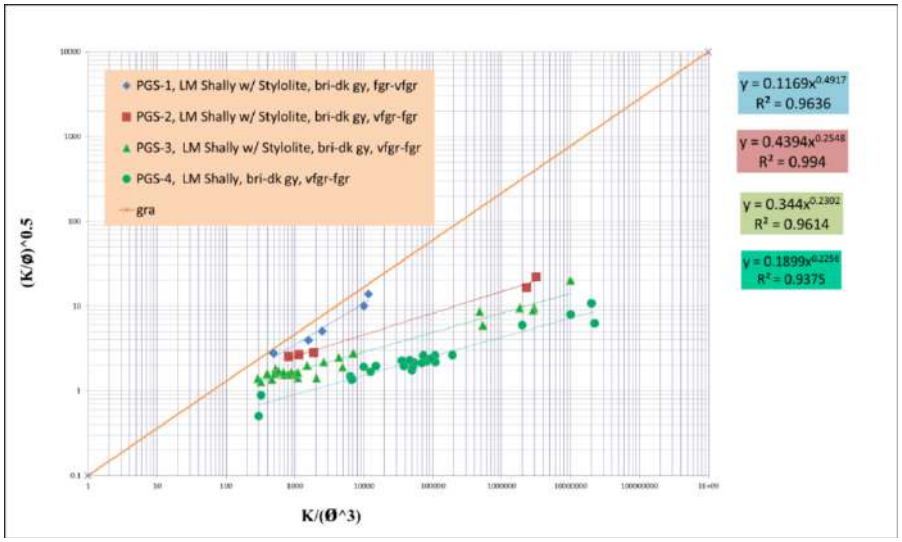

Figure 4. Final Rock Type in the PGS Curve

Based on the plot results from the geometry and pore structure in figure 5, the final rock type is obtained on the PGS curve with 4 groups. Rock Type (RT) 1, dominated by shaly limestone with stylolite, coloured from light-dark grey and grain size from very fine to coarse. RT 2, dominated by shaly limestone with stylolite, dark-light grey, fine to very fine, and carbonated. RT 3, dominated by shaly limestone with stylolite, dark-light grey, fine to very fine, and contains quartz minerals. RT 4, dominated by shaly limestone, dark-light grey, and fine-grained. RT 1 has the highest exponent value of 0.49 and decreases to the lowest value of 0.22 for RT 4. This exponent value represents the form factor and pore size distribution, while the constant does not represent anything. Table 1 is the result of PGS rock type classification and geological description.

To determine the equation between permeability, porosity, and irreducible water saturation it is necessary to substitute the equation between permeability and irreducible water saturation (Sw_{irr}) for each RT equation. By plotting the Sw_{irr} value against k on the semi log curve, the values m and n (constants and exponents) will be obtained.

Table 1. Classification of Rock Type and Geological Descriptions

PGS	Rock Type	Equation	Geological Description
PGS-1	RT-1	$\sqrt{\frac{k}{\emptyset}} = 0.1169 \left(\frac{k}{\emptyset^3}\right)^{0.4917}$	Dominated by shaly limestone with stylolite, coloured from light-dark grey and grain size from very fine to coarse.
PGS-2	RT-2	$\sqrt{\frac{k}{\emptyset}} = 0.4394 \left(\frac{k}{\emptyset^3}\right)^{0.2548}$	Dominated by shaly limestone with stylolite, dark-light grey, fine to very fine, and carbonated.
PGS-3	RT-3	$\sqrt{\frac{k}{\emptyset}} = 0.344 \left(\frac{k}{\emptyset^3}\right)^{0.2302}$	Dominated by shaly limestone with stylolite, dark-light grey, fine to very fine, and contains quartz minerals.
PGS-4	RT-4	$\sqrt{\frac{k}{\emptyset}} = 0.1899 \left(\frac{k}{\emptyset^3}\right)^{0.2256}$	Dominated by shaly limestone, dark-light grey, and fine-grained.

Based on semilog regression on the curve, the value of M (constant) is 0.59 and n (exponent) is 0.14. Previously, the results of the plot size of the grain on the PGS curve produced constants and exponents (a and b) for each rock type. These M, n, a, and b values will be used to calculate the values of A, B, and c using Equations 10, 11, and 12. These values A, B, and c will be used as constants and exponents in the PGS permeability equation. Table 2 is the result of calculating the values of A, B, and c for each rock type.

Table 2. Calculation results for values A, B, and c for each rock type

Rock Type	Equation	*Swirr vs k*	*M*	*n*	*a*	*b*	*A*	*B*	*c*
RT-1	$\sqrt{\frac{k}{\emptyset}} = 0.1169 \left(\frac{k}{\emptyset^3}\right)^{0.4917}$	Swirr = 0.5936 $k^{-0.145}$	0.594	0.145	0.117	0.492	1.983	7.013	2.880
RT-2	$\sqrt{\frac{k}{\emptyset}} = 0.4394 \left(\frac{k}{\emptyset^3}\right)^{0.2548}$	Swirr = 0.5936 $k^{-0.145}$	0.594	0.145	0.439	0.255	1.039	13.523	1.479
RT-3	$\sqrt{\frac{k}{\emptyset}} = 0.344 \left(\frac{k}{\emptyset^3}\right)^{0.2302}$	Swirr = 0.5936 $k^{-0.145}$	0.594	0.145	0.344	0.230	0.828	14.979	2.091
RT-4	$\sqrt{\frac{k}{\emptyset}} = 0.1899 \left(\frac{k}{\emptyset^3}\right)^{0.2256}$	Swirr = 0.5936 $k^{-0.145}$	0.594	0.145	0.190	0.226	0.784	15.285	3.864

Furthermore, to get the final equation the permeability prediction can use Equation 9. The permeability equation which is a function of the porosity and saturation of water is shown in table 3.

Table 3. Final Equations for PGS Permeability Prediction

Rock Type	Final Equation
RT-1	$k = 2.880 \frac{\emptyset^{1.983}}{Sw^{7.013}}$
RT-2	$k = 1.479 \frac{\emptyset^{1.039}}{Sw^{13.523}}$
RT-3	$k = 2.091 \frac{\emptyset^{0.828}}{Sw^{14.979}}$
RT-4	$k = 3.864 \frac{\emptyset^{0.784}}{Sw^{15.285}}$

To get permeability prediction equations that can be applied to wells, PGS distribution can be done using *Interactive Petrophysic* software based on predetermined CT Porosity data. Using the fuzzy logic principle, with input data in the form of CT porosity data and 4 Rock Type groups, namely PGS-1 (RT-1) to PGS-4 (RT-4). In the principle of fuzzy logic, there is a part that needs attention: the number of bins. In this study, the author tries number of bins 5, 10, and 15. The actual approach is bin 5. The results of the PGS distribution are then stored in ASCII format, to be used in calculating the PGS permeability of each CT depth data. The results of the distribution of PGS for Zones 1 and 2 of AY-7 wells are shown in figure 5.

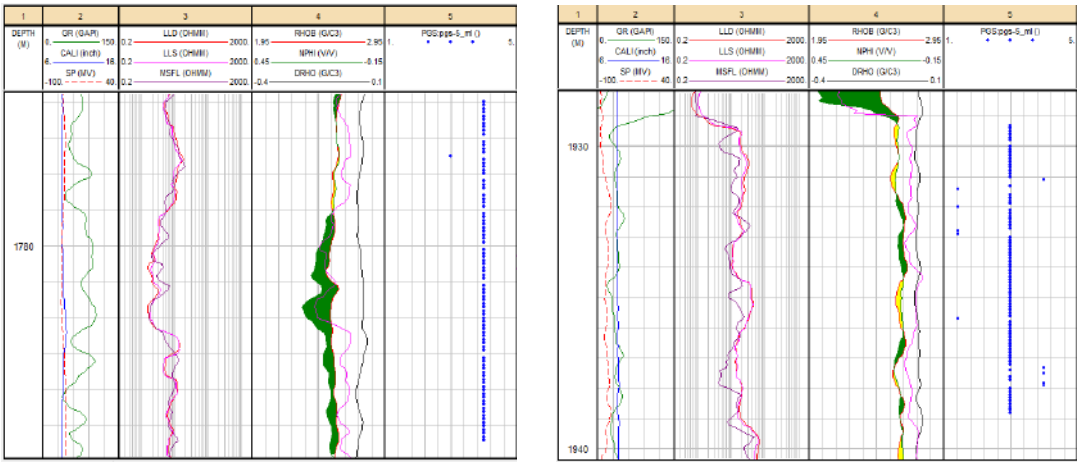

(a) (b)

Figure 5. Results of PGS Distribution of AY-7 Well Data: (a) In Zone 1; and (b) in Zone 2

The PGS distribution that has been done is adjusted to the PGS permeability equation for each rock type. Calculation of PGS permeability can be done using the final equation of PGS permeability prediction. The results of the PGS permeability calculation for Zone 1 and 2 AY-7 wells are shown in Table 4. Based on table 4, the results of the PGS permeability calculation do not differ much or approach the core permeability values. The difference is still within reasonable limits. However, there are still some points that are a little far from the core permeability value.

Table 4. Results of PGS Permeability Calculation Results in AY-7 Well

ZONE 1						ZONE 2					
Depth (m)	*PGS (mD)*	*Core (mD)*	*Depth (m)*	*PGS (mD)*	*Core (mD)*	*Depth (m)*	*PGS (mD)*	*Core (mD)*	*Depth (m)*	*PGS (mD)*	*Core (mD)*
1779.42	0.898	0.91	1782.4	0.072	0.039	1932.34	0.432	0.039	1934.99	0.137	0.047
1779.63	0.063	0.042	1782.6	0.212	0.196	1932.44	3.091	0.41	1935.36	0.249	0.066
1779.9	0.127	0.024	1782.9	3.038	3	1932.54	1.587	0.578	1935.59	0.94	0.528
1780.1	0.154	0.062	1783.24	1.242	1.517	1932.63	24.148	24.161	1935.94	0.135	0.051
1780.4	0.058	0.054	1783.51	0.049	0.063	1932.94	0.033	0.957	1936.26	0.126	0.129
1780.63	6.082	6.069	1783.6	0.29	0.251	1933.01	0.022	2.541	1936.51	0.102	0.097
1780.87	0.226	0.284	1783.86	0.083	0.042	1933.07	0.229	0.15	1936.64	0.768	0.133
1781.3	0.461	0.497	1784.15	0.043	0.032	1933.13	1.431	0.567	1936.82	0.106	0.138
1781.4	0.03	0.031	1784.27	0.019	0.037	1933.49	0.064	0.118	1936.92	0.27	0.515
1781.66	0.021	0.039	1784.4	0.066	0.045	1933.64	0.035	0.085	1938.01	0.152	0.202
1781.9	0.026	0.041	1784.55	0.073	0.062	1933.83	0.061	0.121	1938.12	0.122	0.199
1781.95	0.086	0.07	1785.44	0.032	0.056	1934.4	0.015	0.26	1938.38	0.098	0.206

After obtaining the results of Core, Log, and PGS permeability calculations, the next step is to compare the results of these calculations. The parameters used are porosity and water saturation. For comparison of porosity of CT computation results with core rock data (core) shown in figure 6a, it can be seen that the picture has a pretty good correlation. By performing a regression of the CT and Core porosity data, an equation with an R^2 of 0.90 is obtained. Whereas the correlation between log porosity and core rock porosity is shown in Figure 6b. It can be seen that there are still a lot of log data in the curve away from the core rock value, where the core rock porosity value is used as a reference in validating the accuracy of the calculation results. By performing a log and core porosity data regression plot, an equation with R^2 of 0.63 is obtained. Furthermore, the correlation between log porosity and CT porosity is shown in figure 6c. It can be seen that there are still a lot of log porosity and CT porosity data in the curve. By doing a regression of Log and Core porosity data, an equation with a smaller R^2 value compared to the previous two curves is 0.68.

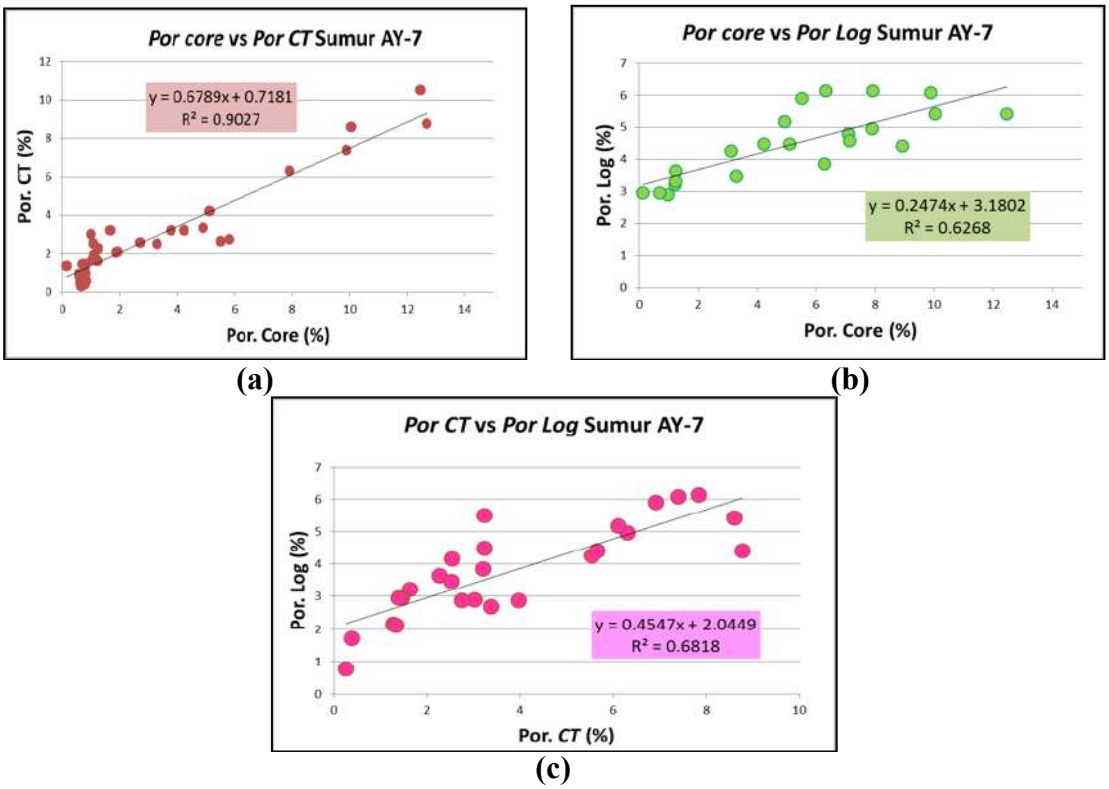

Figure 6. Comparison of Porosity Results in AY-7 Well: (a) Porosity CT vs Porosity Core; (b) Porosity log vs Porosity Core; and (c) Porosity log to Porosity CT

Based on the 3 porosity comparison curves (Figure 6), the porosity value that is close to the calculation results from the laboratory (core data) is CT porosity which shows a good correlation and has a R^2 value that is greater than the curve equation of core porosity to log and porosity of log to CT. This vast difference in value can be caused due to the calculation of the log results, the value taken is the average software calculation results. Whereas in core rocks, data is obtained from the calculation of each rock sample. In the CT calculation results are more specifically obtained by plotting the zones in every 15 points on the core with a length of 1 m. This porosity value will affect the calculation of permeability, where porosity is directly proportional to permeability.

A comparison of the permeability of PGS predictions to core permeability is shown in figure 7a. Can be seen in the figure, the comparison between predicted permeability with core permeability has a good

correlation. The closer the data to the gradient is worth one, the closer the predicted permeability value to the permeability of the core rocks. However, there are some points that move away from one or deviating gradient lines. Obtained R^2 value on the core log permeability regression curve data with PGS permeability is 0.91. Figure 7b is a log permeability comparison curve to PGS permeability. Can be seen, the comparison between log permeability to PGS permeability has a pretty good correlation. However, there is still a lot of data that moves away from one or distorted gradient lines. The value of R^2 obtained is 0.64. Next, figure 7c is the log permeability comparison curve to the permeability of the core rock. Can be seen in the picture below, the comparison between log permeability and core permeability has a correlation that is not good enough. Where there is still a lot of data scattered away from the gradient line with a value of one. R^2 value obtained is small that is equal to 0.84.

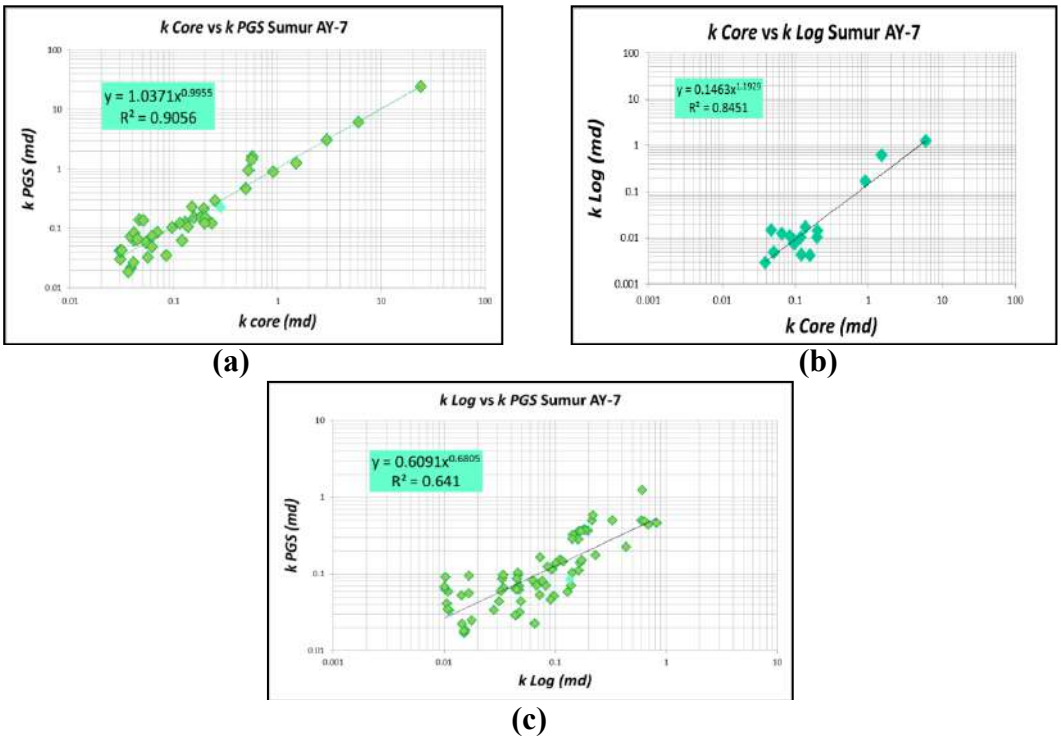

Figure 7. Comparison of Permeability Results in AY-7 Wells: (a) PGS Permeability vs Permeability core; (b) Permeability log vs Permeability core; and (c) Permeability log vs PGS Permeability

Based on the three permeability comparison curves (figure 7), the permeability value close to the results of the calculation of core rock is the PGS permeability shown by good correlation results, the R^2 value is quite large compared to the curve equation of the core permeability to log and log permeability to PGS. Figures 8 and 9 show the final display of the log and PGS permeability calculations.

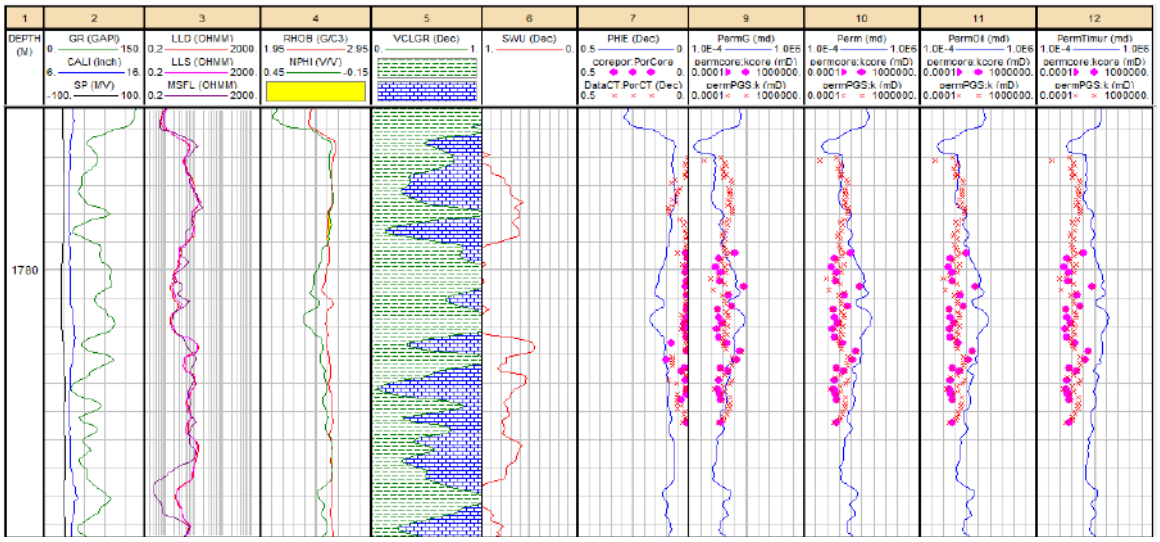

Figure 8. Porosity and permeability comparison of CT, Core, PGS and Log on zone 1 for AY-7 Well

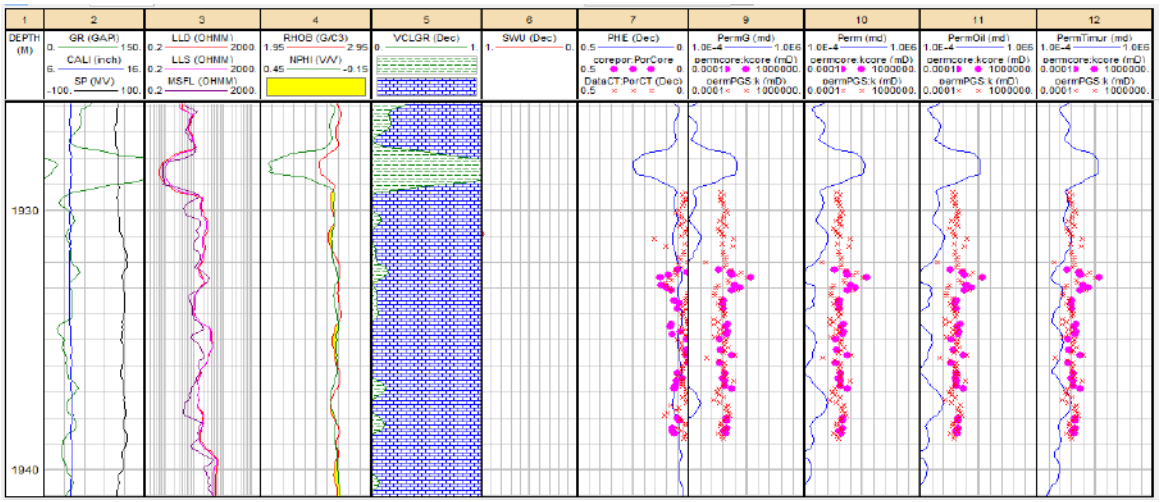

Figure 9. Porosity and permeability comparison of CT, Core, PGS and Log on zone 2 for AY-7 Well

7. Conclusion

The conclusions of this research are: 1) The value of permeability of Core Well AY-7 in this study is an average value of 0.86 mD, with a minimum value of 0.024 mD and a maximum value of 24,16 mD. The average permeability value of PGS AY-7 is 0.89 mD, with a minimum value of 0.01 mD and a maximum value of 24.15 mD. The log permeability value of the AY-7 Well in this study was an average of 0.59 mD, with a minimum value of 0.002 mD and a maximum value of 5,57 mD. Permeability calculation results show that permeability is classified as tight; 2) Based on the results of core, log, and PGS permeability calculations, the permeability values close to the results of calculations from the laboratory (core data) are PGS permeability.

8. References

[1] Darman, H. dan Sidi, F. H. 2000. An Outline of The Geology of Indonesia. *Makalah Ikatan Ahli Geologi Indonesia (IAGI)*. Vol 20th. Indonesia.

[2] Demir, M. dan Demiral, B. 2001. Effect of Pore Size Distribution On Porosity Measurement By Computerized Tomography. *Paper Society of Core Analysis.* SCA 2001-49.

[3] Dewanto, O., Mulyatno, B.S., Rustadi and Wibowo, R.C. 2017. Determining the Temperature of Shale Material Conversion Into Crude Oil Based on Organic Clay and Organic Carbonate Test Outside Reservoir. *International Journal of Mechanical and Mechatronics Engineering, IJMME*. Vol:17 No:05. ISSN: 2077-124X (Online), 2227-2771 (Print). Page: 84-89.

[4] Gardner, W.R., 1958. Some Steady State Solutions Of The Unsaturated Moisture Flow Equation With Application To Evaporation From A Water Table. *Soil Science*. 85: 228-232.

[5] Harsono, A., 1994. *Teknik Evaluasi Log*. IATMI. Schlumberger Data Services. Jakarta.

[6] Irawan, D. dan Utama, W., 2009. Analisis Data *Well Log* (Porositas, Saturasi Air, dan Permeabilitas) untuk Menentukan Zona Hidrokarbon, Studi Kasus: Lapangan "ITS" Daerah Cekungan Jawa Barat Utara. *Jurnal Fisika dan Aplikasinya* vol. 5, No.1. Surabaya: Institut Teknologi Sepuluh November.

[7] Koesoemadinata, R.P., 1980. *Geologi Minyak dan Gas Bumi*. Bandung: Institut Teknologi Bandung. 296 p.

[8] Listiyowati, L.N., 2018. Perbandingan Analisis Porositas Porites Menggunakan Teknik Micro-CT dan Optik. *Riset Geologi dan Pertambangan*, vol. 28, No.1 (91-100). Bandung.

[9] Permadi, P., and Susilo, A. 2009. Permeability Prediction and Characteristics of Pore Structure and Geometry as Inferred from Core Data. *Paper Society Petroleum Engineers (SPE) 125350-PP*. Abu Dhabi.

[10] Permadi, P. dan Wibowo, A.S., 2013. Kozeny's Equation For Better Core Analysis. *Paper Society of Core Analysis* (*SCA*) *2013-048*. International Symposium of The Society of Core Analysis. Napa Valley, California.

[11] Sinclair, S., Gresko, M., and Sunia, C., 1995. Basin Evolution of the Ardjuna Rift System and its Implications for Hydrocarbon Exploration, Offshore Northwest Java, Indonesia. *Indonesian Petroleum Association (IPA) Proceedings*, 24th, hal 147-162. Annual Convention, Jakarta.

[12] Yogi, A. 2018. Estimasi Permeabilitas dengan Beberapa Metode Karakterisasi Reservoar Untuk Formasi Talang Akar. *Jurnal Lembaga Publikasi Minyak dan Gas Bumi*, Vol. 52 No.1, April 2018 : 3-5. Jakarta Selatan: PPPTMGB LEMIGAS.

Acknowledgment

The author would like to thank all those who have helped by providing useful direction, discussion and support during the course of this research.